SK/
JDF

NASA Technical Paper 1607

Stress Analysis and Buckling of J-Stiffened Graphite-Epoxy Panel

Randall C. Davis

FEBRUARY 1980

NASA

NASA Technical Paper 1607

Stress Analysis and Buckling of J-Stiffened Graphite-Epoxy Panel

Randall C. Davis
Langley Research Center
Hampton, Virginia

National Aeronautics
and Space Administration

**Scientific and Technical
Information Office**

1980

SUMMARY

A graphite-epoxy shear panel with bonded-on J-stiffeners has been investigated. This panel was loaded to buckling in a picture frame shear test. Two finite element models, each of which included the doubler material bonded to the panel skin under the stiffeners and at the panel edges, were used to make a stress analysis of the panel. The shear load distributions in the panel from two commonly used boundary conditions, applied shear load and applied displacement, were compared with the results from one of the finite element models that included the picture frame test fixture. Analysis results show that use of the bonded doubler material under the stiffeners and at the panel edges in conjunction with the test fixture loading produces a highly nonuniform shear load distribution in the panel. The analytical results were verified by comparison with strain and buckling results from the well-controlled laboratory test of the panel.

INTRODUCTION

In experimental practice, simple methods are commonly used for reducing shear data. With these methods, measured experimental values such as load, displacement, and strain are related by simple analytical expressions. Basic to most of these expressions is the assumption of a uniform shear load distribution throughout the panel.

Establishing a state of uniform inplane shear in a test specimen is difficult to achieve in an experiment. Many different test procedures have been used for studying the shear stiffness and buckling strength of composite panels. The advantages and disadvantages of these procedures are discussed in references 1 to 7. The picture frame shear test is one such procedure that has been widely used in the laboratory to assess the shear strength and buckling of complex composite hardware. A rectangular picture frame was used in this investigation to test a conceptual composite panel (see figs. 1 to 3) for the empennage of a commercial transport (ref. 8). The design of the test panel allowed elastic skin buckling to take place locally; stiffeners forced the general instability mode to occur at a load level much higher than that for local skin buckling.

Unlike concepts where stiffeners are attached to the panel with rivets, this panel uses stiffener flanges and doubler material bonded to the panel skin which can contribute significantly to the shear stiffness of the panel and can cause a highly nonuniform shear load distribution in the panel. Some investigators account for extra stiffening effects experimentally by cutting out the skin portion of the panel specimen. They then test the specimen edge-stiffening material separately to determine the shear stiffness of the bonded doubler material to be considered in subsequent data reductions. The shear test frame components may also affect the uniformity of the load introduced at the panel edges. The combined effect of the bonded doubler material and test frame loading was taken into account in the analytical model for this investigation.

Strains obtained using detailed finite element models were compared with strains obtained experimentally. The buckling strains for the panel were then computed by means of a simpler analysis code and were compared with buckling strains obtained experimentally. Excellent agreement between test and theory was obtained for both the load distribution in the panel and the buckling load.

SYMBOLS

P tensile load applied to corners of picture frame test apparatus, N

x coordinate across panel width, cm

y coordinate along length of panel, cm

γ shear strain

Subscript:

s symmetric

EXPERIMENTAL INVESTIGATION

Dimensions of the graphite-epoxy shear panel specimen and frame are given in figures 1 to 3. The panel consists of a 34.29- by 59.69-cm, 6-layer $[90/\pm45]_s$, laminated panel skin to which J-section stiffeners are bonded. The ends of the longitudinal stiffeners are closed off with transverse J-stiffeners, all of the same layup and dimensions. Because the stiffener flanges are turned inward on either side of the longitudinal center line and at the ends, the panel is symmetric about both its longitudinal and transverse axes.

The panel was tested in a tensile load machine where the picture frame apparatus converts the tensile load to a shear strain on the specimen. The panel was first pulled from one set of diagonally opposite corners, as shown in figures 4 and 5, and this loading was designated the positive shear loading. The panel was then removed from the test machine, loading yokes were placed in the other two corners, and the panel was retested. This latter loading was designated the negative shear loading. Differences between the test results for these two loadings were used to determine the anisotropic effects of the 6-ply panel skin layup on the shear buckling load. To assess repeatability of the buckling loads, the panel was tested a third time in a negative load position and a fourth time in a positive load position.

Test Specimen Geometry

Details of the various ply orientations for the panel are given in figure 2. The J-stiffeners have 4-ply $[\pm45]_s$ webs and 6-ply $[0/\pm45]_s$ outer flanges. Cocuring the stiffener with the panel skin results in a 10-ply layup on each side of the interior stiffener centers. (See fig. 2(b).) The 4-ply $[0_2/\pm45]$ part of this 10-ply layup for the two inner stiffeners tapers to zero

in equal steps away from the stiffener centers over a 1.52-cm length for the two inner stiffeners. For the edge stiffeners, this tapering takes place in equal steps over a 0.89-cm length and includes the tapering of an additional 4-ply [45/0/-45/90] doubler on the skin side of the panel. The outer edges of the panel skin have a doubler that forms a 22-ply edge layup. (See fig. 2(a).) The lamina properties for the panel plies are given in table I.

Figures 3 to 5 illustrate the method of load introduction for the test panel. The panel edges were attached to the heavy steel frame bars by means of thin gage (0.081-cm-thick) aluminum load introduction strips as shown in figure 3. These load introduction strips ensured that neither bending nor loads normal to the inplane shear load were applied to the edges of the panel. Ten equally spaced aluminum cross braces, 2.54 by 1.90 cm in cross section, were used between the long edges of the panel to force these edges to remain parallel during the test. (See fig. 5.)

The diagonals of the shear specimen and the picture frame were misaligned geometrically by more than 3°. (See fig. 6.) Consequently, decomposing the applied tensile force P into components parallel to the panel edges leads to two conflicting values for the shear resultant. Moment equilibrium must be preserved during loading; the specimen, therefore, rotates within the available clearances because the load introduction strips offer little resistance to this motion. To avoid the conflicting shear resultants, the applied shear resultant for this report was calculated by dividing the applied tensile load P by the diagonal length of the panel.

Test Procedure

The panel was instrumented with back-to-back strain gage rosettes at various locations on the panel skin as can be seen in figures 4 and 5. Strain values were recorded with increasing load by an automated data acquisition system. The shear strain γ was calculated according to the rosette relations given in reference 9.

At buckling, rosettes on one side of a buckled section showed an increase in γ with load, while rosettes on the other side showed a decrease in γ with increasing load. The plot in figure 7 shows the shear strain reversal results for the negative shear test. Strain gage rosettes for this plot were located on opposite sides of the panel near the specimen center. The strain reversal point on the curve is defined as the point where the maximum shear strain γ accrued before decreasing with load. Furthermore, of all the strain reversals given by the various rosettes, the reversal point which occurred at the lowest load level was used to determine the shear buckling load.

A moiré fringe grid was used to determine the local buckle pattern. The load at which the buckle waves were first observed during tests was very close to the buckling load found from the strain reversal plots. The experimental half-wavelengths shown in table II were determined by dividing the panel length by the number of fully developed half-waves visually observed in the central section.

ANALYTICAL INVESTIGATION

The effect of the bonded doubler material and the picture frame load on the panel shear load distribution and buckling load was studied analytically. Details of the analytical methods and the modeling refinements are described below.

Stress Analysis

Two finite element models were constructed for analysis using the SPAR computer code (ref. 10). The first model was constructed for investigating the difference in stress distribution between a uniform applied shear load and a uniform applied displacement boundary condition. The second model was constructed to determine the effect of the loading frame on the stress distribution. The models included the details of the bonded doubler material under the stiffeners and at the panel edges. The stiffener web and outside flange are not considered to contribute significantly to the shear stiffness and, therefore, to reduce computational costs, were not included in the finite element models.

The edges of the first SPAR panel model were treated as essentially simply supported; that is, the edge rotations were unconstrained and the out-of-plane displacements were restrained to zero. In the first boundary condition case, a uniform shear load was applied to all the edges. In the second boundary condition case, the long edges were given a specified tangential displacement and the ends were constrained in the transverse direction. An equivalent shear load for the applied displacement case was found by integrating the shear load resultant curve along the plane edge and dividing by the panel length. For comparison purposes, the magnitude of the applied displacements was adjusted so that the average shear resultant for the long edge of the panel equaled the shear resultant applied for the uniform edge-loading case.

The second SPAR finite element model was constructed to determine the influence of the aluminum load introduction strips and the steel picture frame bars on specimen stress distribution and stiffness. The second model had the same panel details as the first and, in addition, included the steel frame bars and the aluminum load introduction strips shown in figure 3. The steel picture frame bars were modeled as single inplane plate elements. The pinned corners of the frame were duplicated by using a pinned-end condition in the model at the intersection of the bars of the picture frame at the corner pin locations. The SPAR code enforces displacement compatibility at these corner junctions without introducing any inplane bending, just as the corner pins do in the actual test hardware.

The steel frame bars and panel dimensions in the second model were matched to the actual planar specimen dimensions so as to include the effect of the misaligned diagonals of the panel and frame. The aluminum load introduction strips were modeled as one double thickness, inplane plate element with a shear stiffness equal to the shear stiffness of aluminum; the other stiffnesses were set at zero.

Shear Buckling Analysis

Buckling strains for the panel were computed using VIPASA (ref. 11), a linked-plate eigenvalue analysis code. The panel cross section was modeled in detail to accurately include the effect of the bonded doubler material under the stiffeners on the buckling mode. In the VIPASA model, a separate plate was used for each segment of the tapered doubler section where a layer was truncated. The junction of two plates of unequal thickness but with a common reference surface was accomplished by using offsets. The analysis, however, cannot include the effect of stiffeners that run across the cross section at the panel ends. The frame was not included in the model and the applied shear load was uniform.

One limitation of the VIPASA shear buckling analysis is that the ends of the panel are treated as if the panel were infinitely long. For the analyses presented here, the buckling wavelengths were small in comparison to the panel dimensions; therefore, the effect of this limitation of the code is not considered important. The lateral edges, however, can have any prescribed boundary condition. The 22-ply outer edges of the panel were very stiff in comparison to the 6-ply skin and, therefore, use of clamped or simply supported boundary conditions for the edge had a negligible effect on the buckling results. For this report, buckling strains were obtained with the edges treated as simply supported.

RESULTS AND DISCUSSION

This section presents the experimental and analytical results and discusses the correlation of experiment and theory.

Experimental Buckling Results

The experimental buckling load results are given in table II. Of the four tests run, the buckling loads from the third and fourth indicated that the panel tests were highly repeatable. The local buckling loads for the positive shear configuration from the first and fourth tests were within 2 percent of each other; the negative shear buckling loads from the second and third tests demonstrated the same repeatability. Consequently, the results from the first and second tests only are reported.

For a panel skin of only 6 plies, the ±45 plies can produce a significant anisotropic effect on shear buckling behavior. Experimental results presented in table II indicate that anisotropy raises the positive shear buckling load 27 percent above the negative shear buckling load.

Analytical Results

The shear load distributions for the two SPAR models are shown in figures 8 to 10. Results for the first model are shown by the dashed curves; the second model results are shown by the solid curves. The ordinate shows

the shear resultant normalized by the applied shear load, and the abscissa shows the position along the panel normalized by the panel length of 59.69 cm or by the panel width of 34.29 cm. The normalizing shear load in each loading case is the tensile load divided by the panel diagonal length (as discussed in the section on specimen geometry). The tensile load for the two edge conditions on the first SPAR model is the magnitude of the vector sum of the edge loads. For the displacement edge condition, the edge loads were found by integration (as discussed in the section on stress analysis). In the second SPAR model analysis, the tensile load is the load applied at the corners of the model. Thus, the resulting analytical shear load distributions from the first and second panel models (figs. 8 to 10) can be compared directly on the basis that they both have the same applied tensile load P.

The stress analysis results for the first SPAR model of the panel (fig. 8) show that the shear load distribution introduced along the panel edge was strongly influenced by the manner in which the load was applied. When a uniform shear load was applied to all edges of the panel, the load distribution throughout the panel was fairly uniform and almost equal to the applied load. When a uniform displacement was applied, however, the uniformity of the shear load distribution along the edge and at the center of the panel was greatly affected by the presence of the stiffening material, as can be readily seen in figure 8. The small deviations in the normalized edge load from 1.0 for the uniform load case seen in figure 8 result from the analysis code and the element mesh spacing chosen for the outer edge of the panel. These deviations are insignificant because they are well within the scope of accuracy sought for this analysis.

The SPAR stress analysis results for the second model demonstrate that the frame and load introduction strips have a profound effect on the load distribution introduced to the outer edges of the panel. The most obvious effect seen in figure 8 is the lack of uniformity in load introduction. The results also indicate that the load introduced at the panel edge is not symmetric with respect to the panel length.

The shear load distribution in the interior of the panel is shown in figures 9 and 10. The two edge conditions give a fairly uniform distribution in the panel except near the edges. The second SPAR model also shows a uniform shear load distribution over most of the panel interior. The two SPAR model results differ primarily in the magnitude of the shear load over most of the interior of the panel. Results from the second SPAR model analysis show a 23-percent reduction in the magnitude of the shear resultant at the center of the panel compared to a uniformly distributed shear load in the first SPAR model analysis.

The results of the VIPASA buckling analysis illustrate that the stiffeners do not participate in the buckling displacements. The line showing the intersection of the stiffener with the panel skin remains straight during local buckling. Thus, the buckle waves are confined to the region between stiffeners and have a wavelength, shown in table II, approximately that of the stiffener spacing. Consequently, the nonuniformities in the shear load near the panel edges have very little effect on the buckling strains in the panel skin between the interior stiffeners.

Comparison of Test and Theory

According to the stress analysis performed with the second SPAR finite element model, a large portion of the center of the panel is subjected to a uniform reduced level of shear loading. The accuracy of this stress analysis is verified by the excellent agreement between the second SPAR model results and test data as shown in figures 9 and 10. The uniformity of the shear load in the central portion of the panel permits calculation of a buckling strain using the linked-plate analysis code. This code accurately models the tapered doubler material under the stiffeners which significantly affects the local buckling strain.

The buckling strains were used in conjunction with the SPAR stress analysis results in figure 11 to determine the tensile load needed to buckle the panel. The VIPASA strains, marked off on the strain axis in figure 11, when extended upward, intersect the SPAR stress analysis curve to give the analytical tensile load required to buckle the panel. The positive (+) and negagive (-) shear buckling tensile test loads determined in this manner are listed in table II as SPAR results using VIPASA strains. As can be seen, these loads are 1.04 and 0.99 times the positive and negative experimental values, respectively.

CONCLUDING REMARKS

The picture frame test apparatus and the presence of bonded doubler material around the panel edges and under the stiffeners cause a highly non-uniform shear load to be introduced at the panel edges. A structural analysis which ignores the influence of the test frame and the bonded doubler material results in a 23-percent error in predicting the internal shear loads. To predict the internal shear load accurately, the complete panel and frame must be analyzed using a two-dimensional structural analysis code.

An eigenvalue analysis which accounts for the interaction between the panel skin and bonded doubler material can be used to predict accurate local buckling strains. These buckling strains can be related to the applied tensile load by using the stress analysis from a two-dimensional model. Buckling loads determined in this manner agree within a few percent of test results.

Langley Research Center
National Aeronautics and Space Administration
Hampton, VA 23665
January 17, 1980

REFERENCES

1. Tarnopol'skiy, Yu. M.; and Kintsis, T. Ya.: Static Methods of Testing Reinforced Plastics. NASA TT F-16669, 1976.

2. Bergner, Henry W.; Davis, John G., Jr.; and Herakovich, Carl T.: Analysis of Shear Test Method for Composite Laminates. VPI-E-77-14, Virginia Polytech. Inst. & State Univ., Apr. 1977. (Available as NASA CR-152704.)

3. Composite Materials: Testing and Design. Spec. Tech. Publ. 460, ASTM, 1969.

4. Jones, Robert M.: Mechanics of Composite Materials. McGraw-Hill Book Co., c.1975.

5. Bush, Harold G.; and Weller, Tanchum: A Biaxial Method for Inplane Shear Testing. NASA TM-74070, 1978.

6. Weisshaar, Terry A.; and Garcia, Ramon: Analysis of Graphite/Polyimide Rail Shear Specimens Subjected to Mechanical and Thermal Loading. NASA CR-3106, 1979.

7. Garcia, Ramon; Weisshaar, T. A.; and McWithey, R. R.: An Experimental and Analytical Investigation of the Rail Shear-Test Method As Applied to Composite Materials. J. Exp. Mech., 1980. (To be published.)

8. Lehman, George M.: Development of an Advanced Composite Rudder for Flight Service on the DC-10. Third Conference on Fibrous Composites in Flight Vehicle Design - Part I, NASA TM X-3377, 1976, pp. 71-91.

9. Hetényi, M., ed.: Handbook of Experimental Stress Analysis. John Wiley & Sons, Inc., c.1950.

10. Whetstone, W. D.: SPAR Structural Analysis System Reference Manual - System Level 13A. Volume I: Program Execution. NASA CR-158970-1, 1978.

11. Anderson, Melvin S.; Hennessy, Katherine W.; and Heard, W. L., Jr.: Addendum to Users Guide to VIPASA (Vibration and Instability of Plate Assemblies Including Shear and Anisotropy). NASA TM X-73914, 1976.

TABLE I.- MATERIAL PROPERTIES USED IN ANALYSIS

Lamina thickness, cm	0.014
Modulus in fiber direction, GN/m^2	131.0
Modulus in transverse direction, GN/m^2	13.0
Lamina shear modulus, GN/m^2	6.41
Poisson's ratio	0.310

TABLE II.- BUCKLING RESULTS

	Buckling load for panel, kN	Buckling half-wavelength, cm	Buckling shear strain
SPAR with VIPASA strains:			
Positive shear	27.78	7.37	0.00152
Negative shear	20.79	6.60	0.00114
No anisotropy	24.47	6.60	0.00134
Experiment:			
Positive shear	26.71	7.37	0.00147
Negative shear	21.00	7.37	0.00117

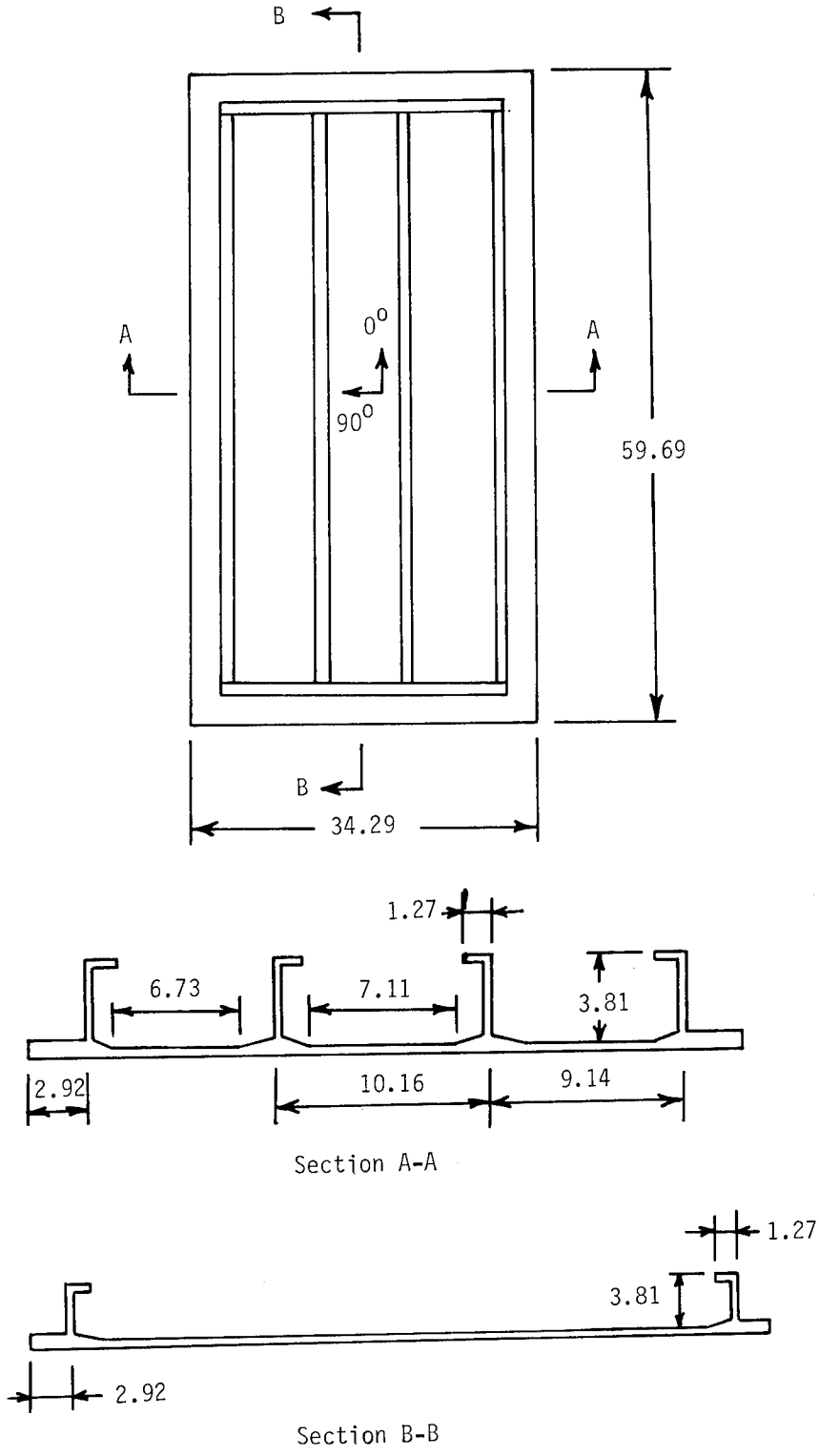

Figure 1.- Schematic details of panel geometry (dimensions in centimeters, not to scale).

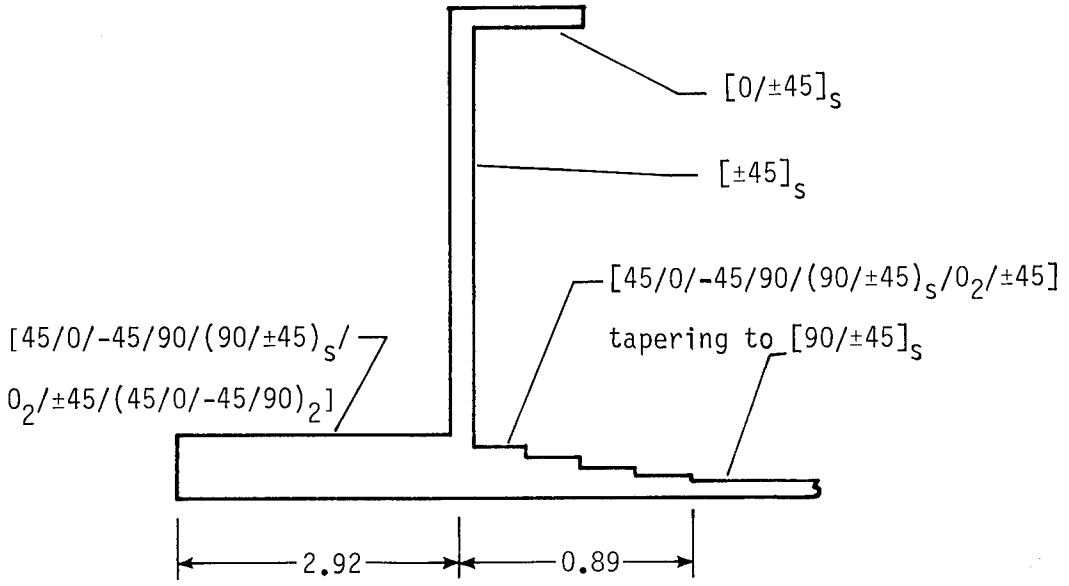

(a) Layup details of edge J-stiffener.

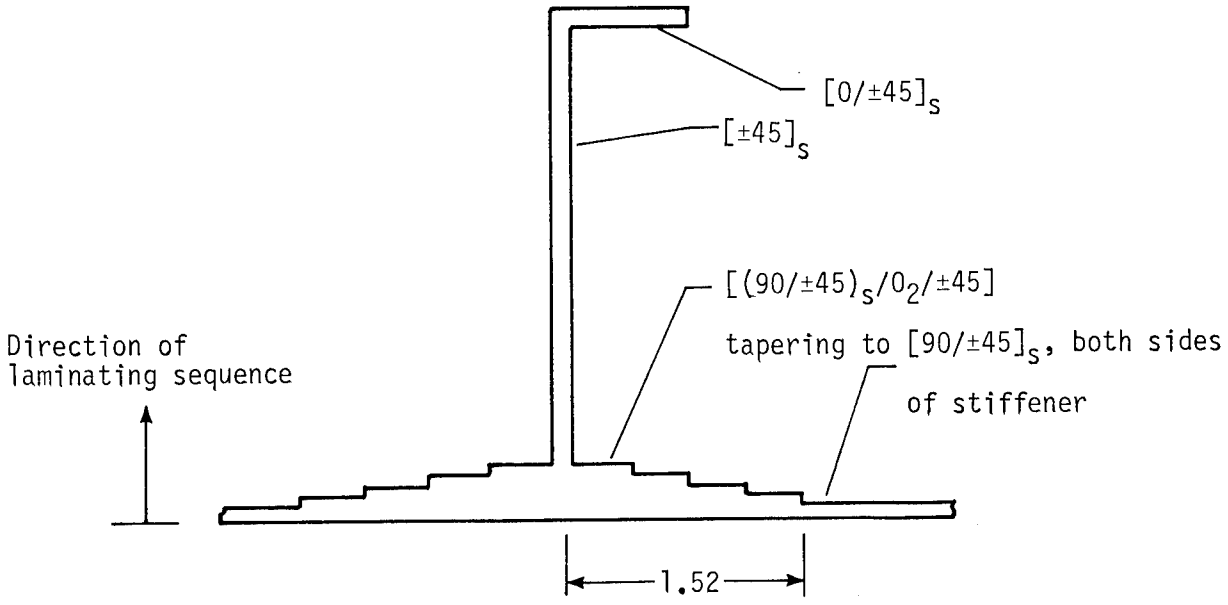

(b) Layup details of interior J-stiffener.

Figure 2.- Layup details of J-stiffeners (dimensions in centimeters).

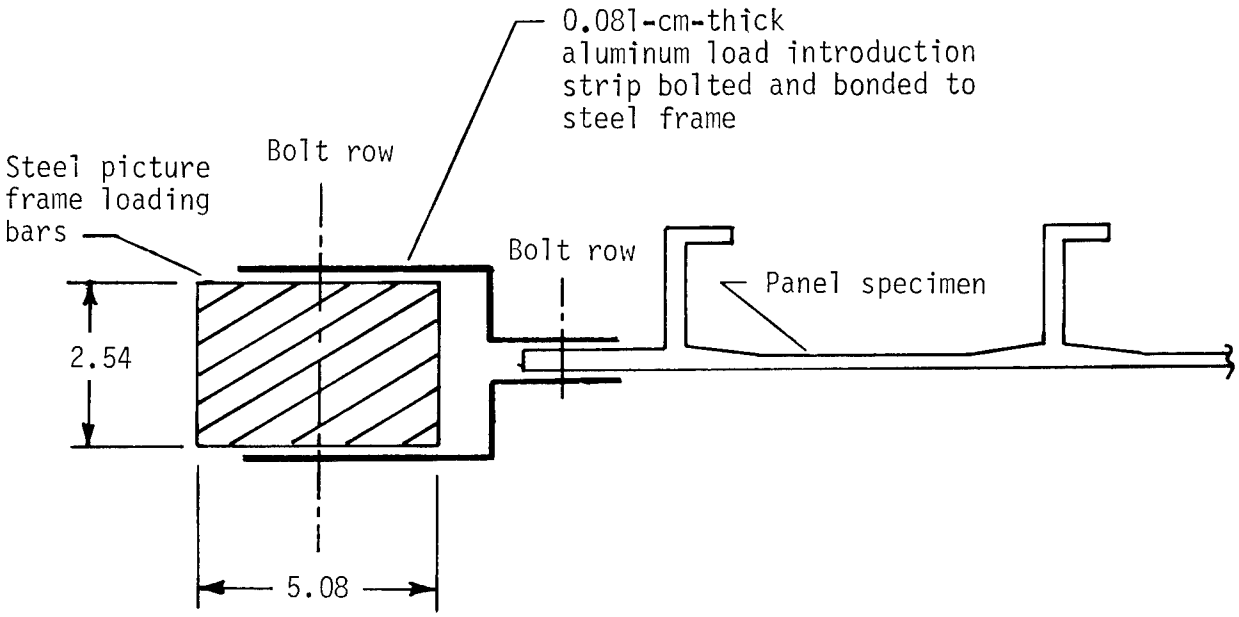

Figure 3.- Details of load introduction method (dimensions in centimeters).

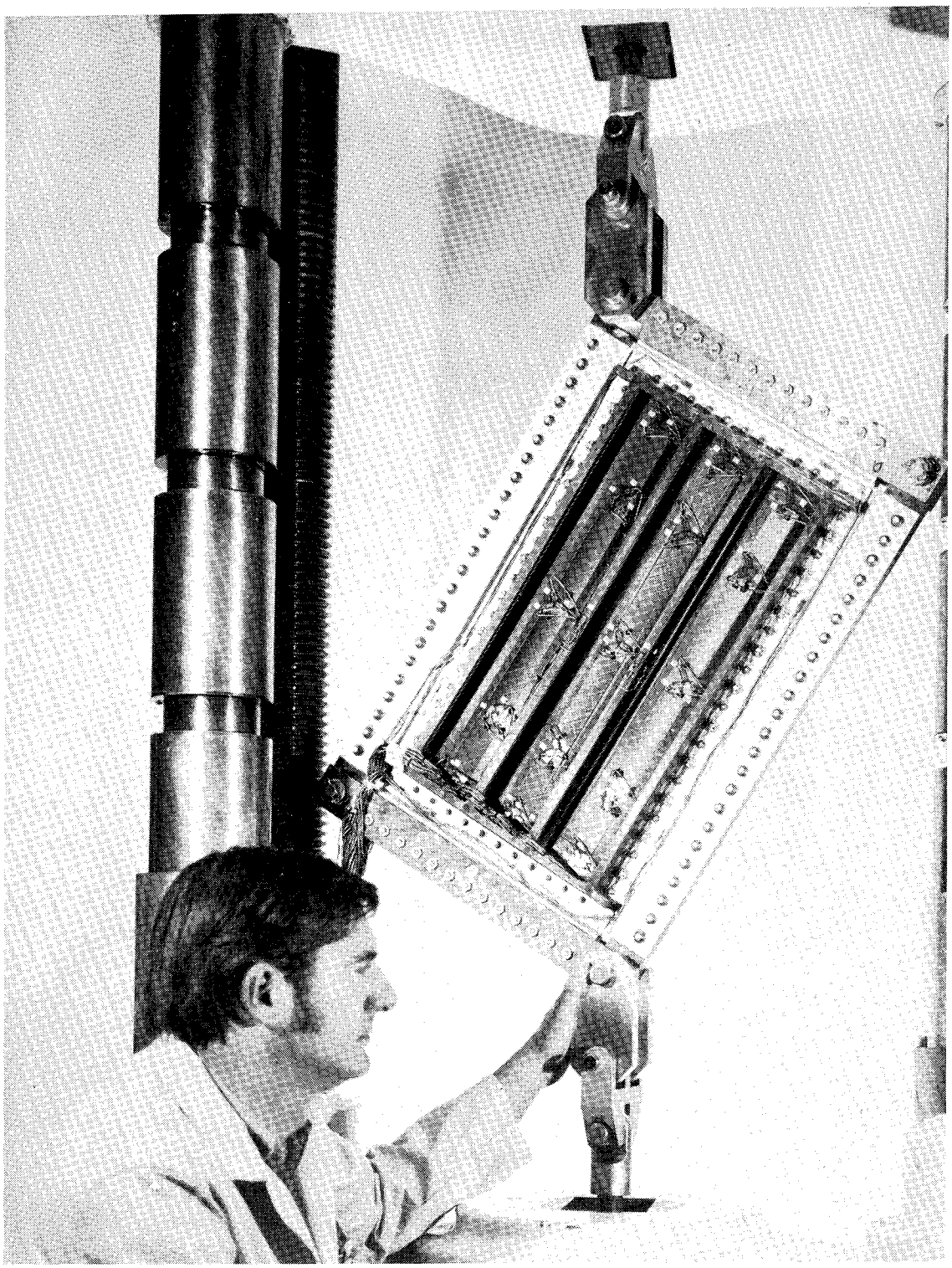

L-80-101

Figure 4.- Front view of test panel.

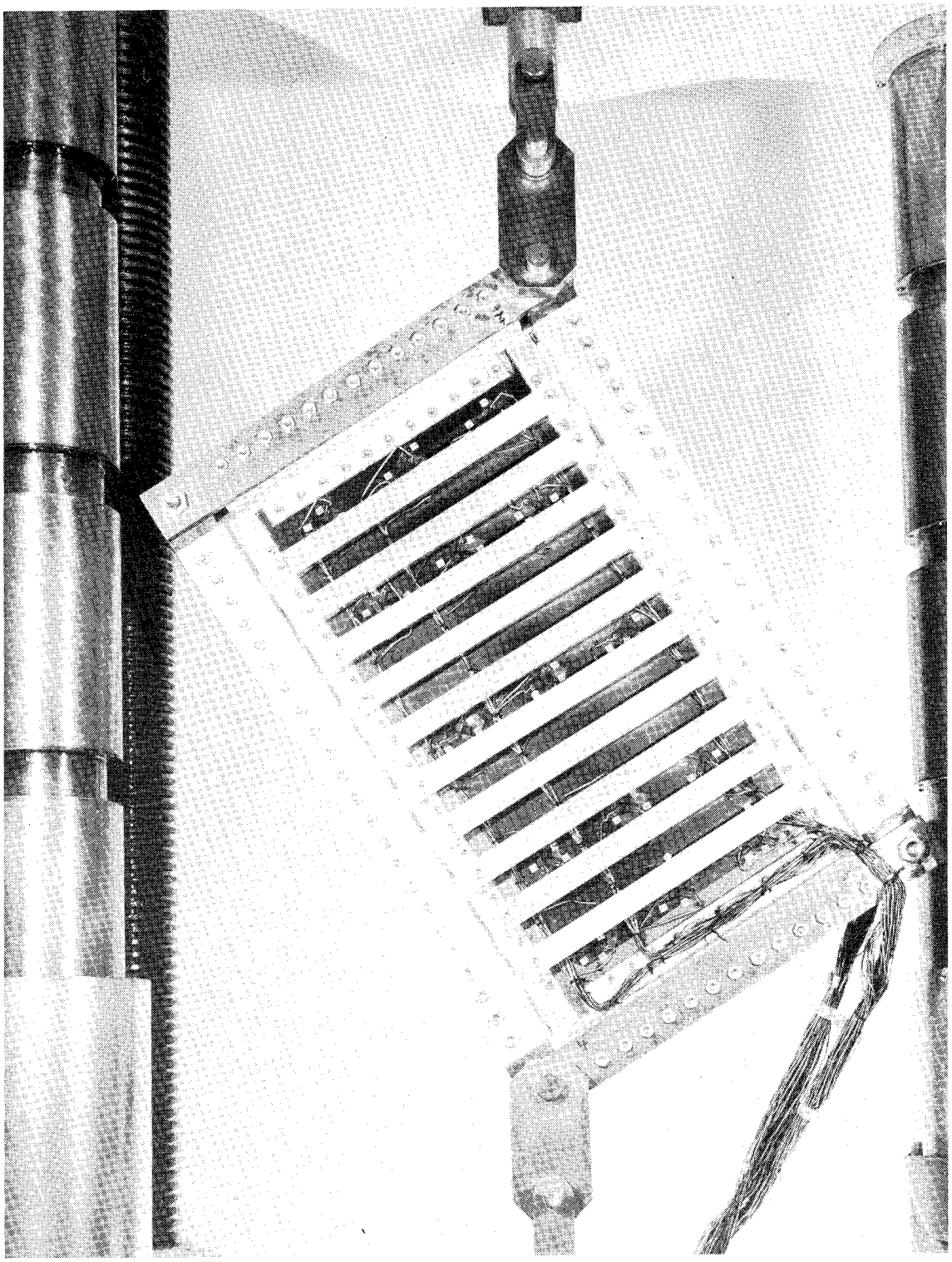

L-80-102

Figure 5.- Back view of test panel.

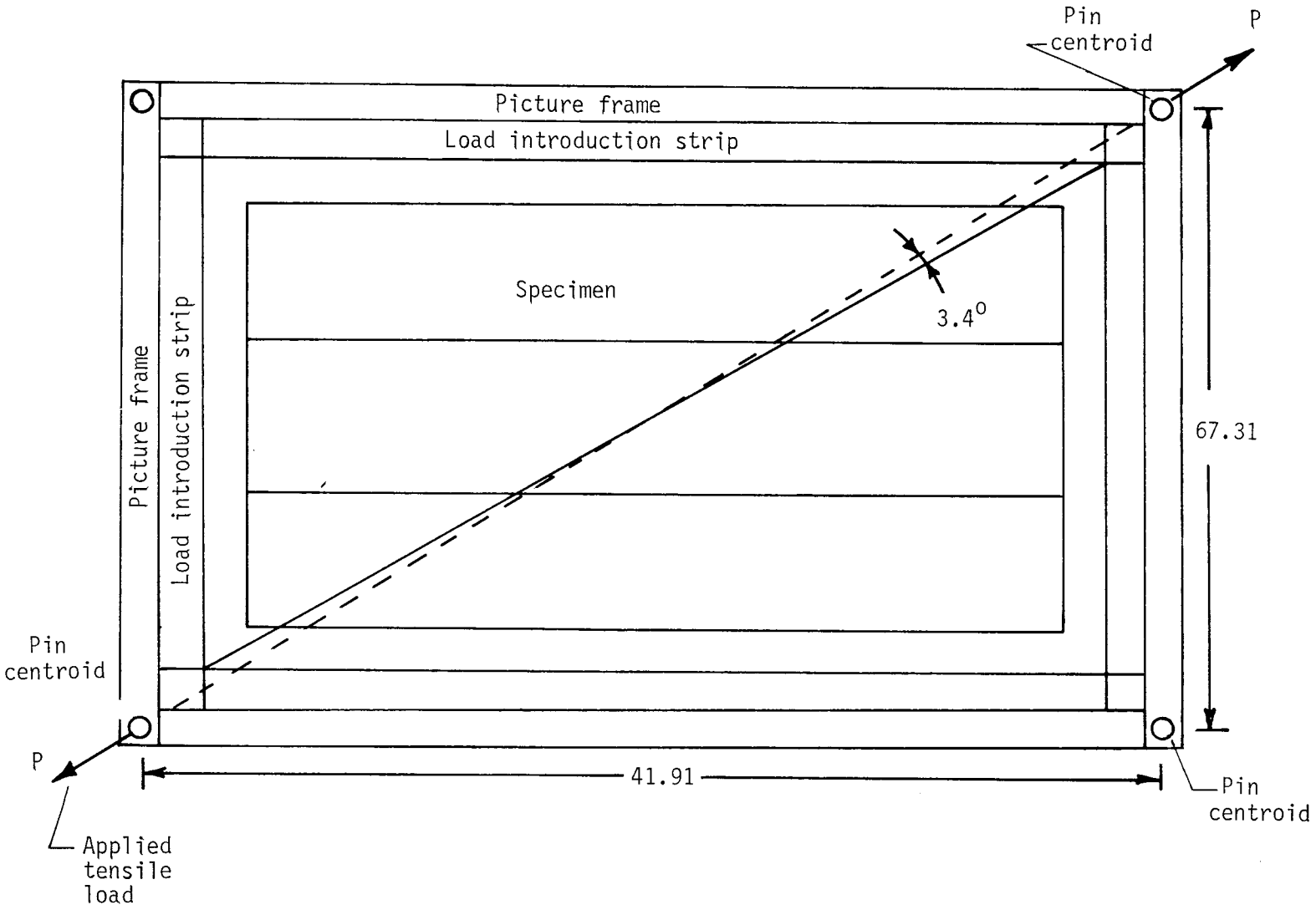

Figure 6.- Schematic of picture frame shearing apparatus (dimensions in centimeters).

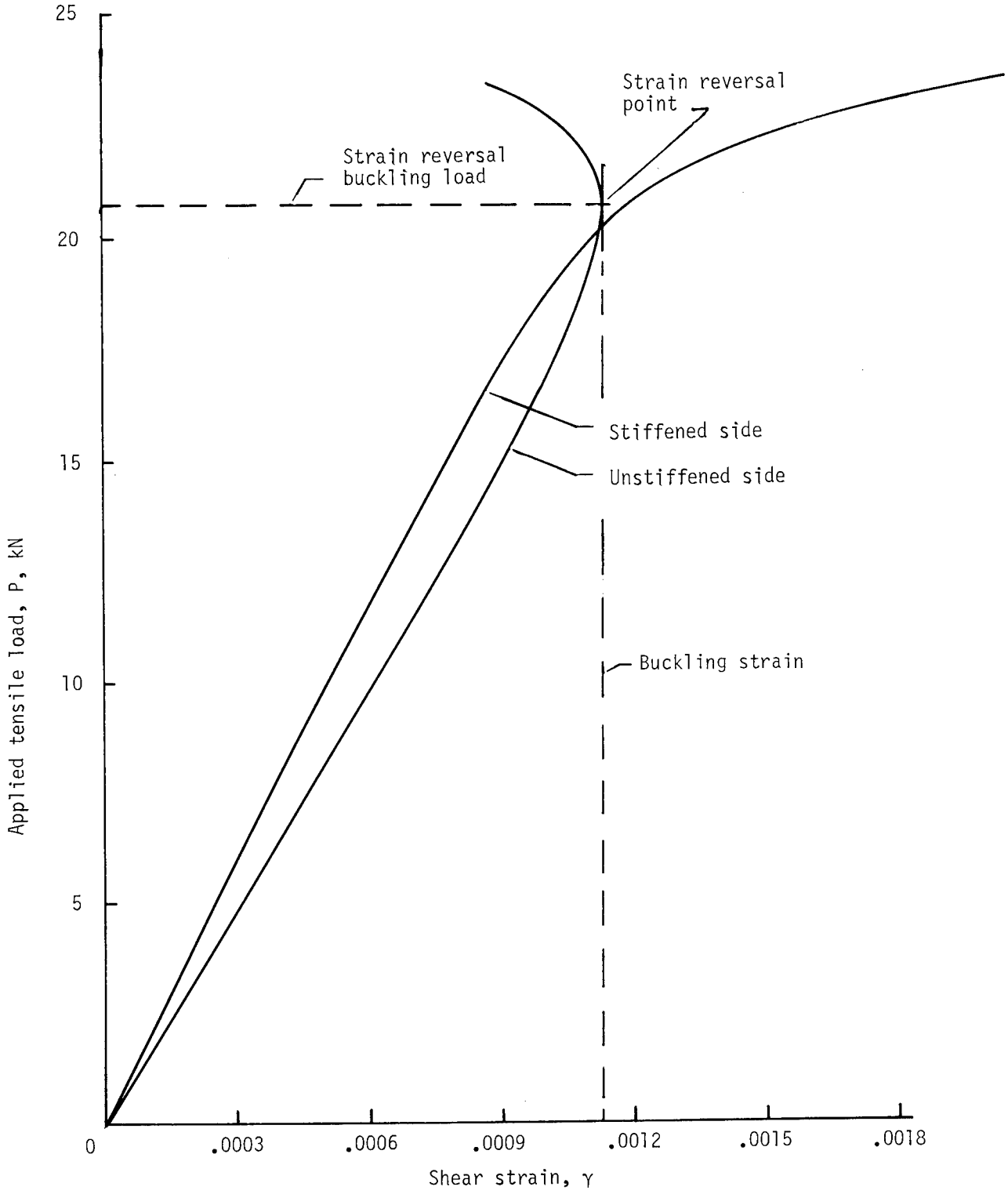

Figure 7.- Load-strain plot showing strain reversal at buckling for negative shear test.

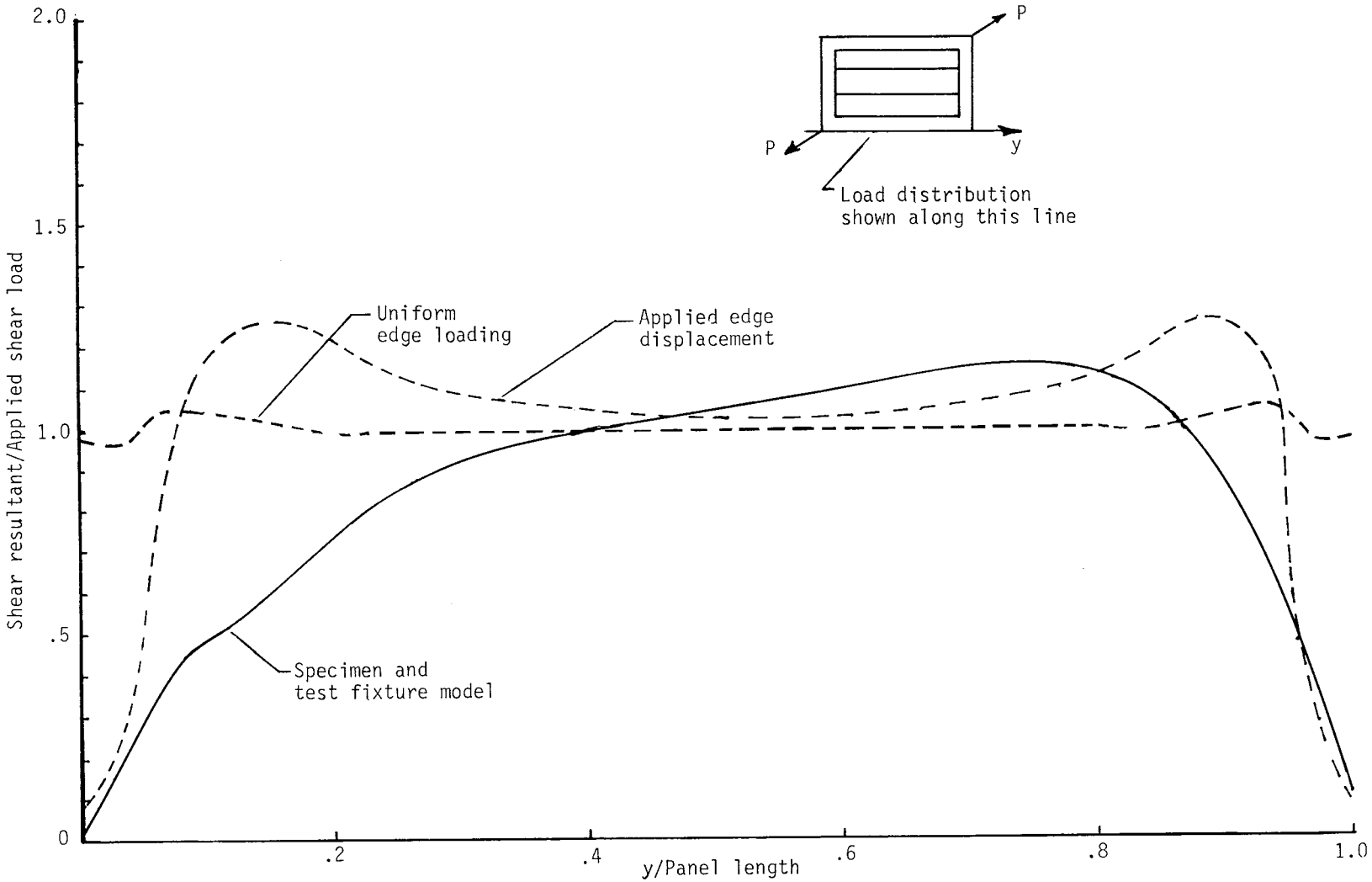

Figure 8.- Shear load distribution along long edge of panel.

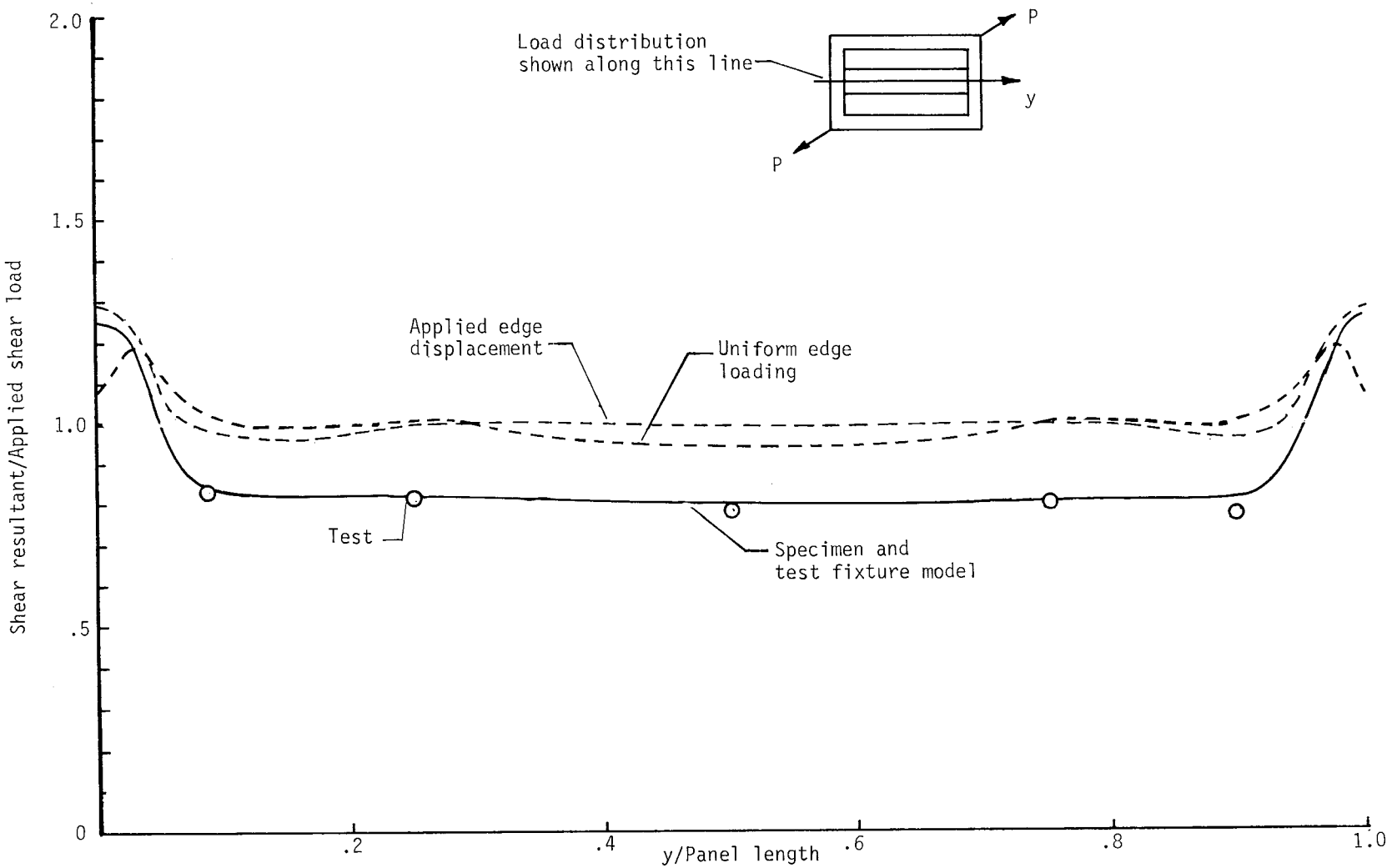

Figure 9.- Shear load distribution along center section of panel.

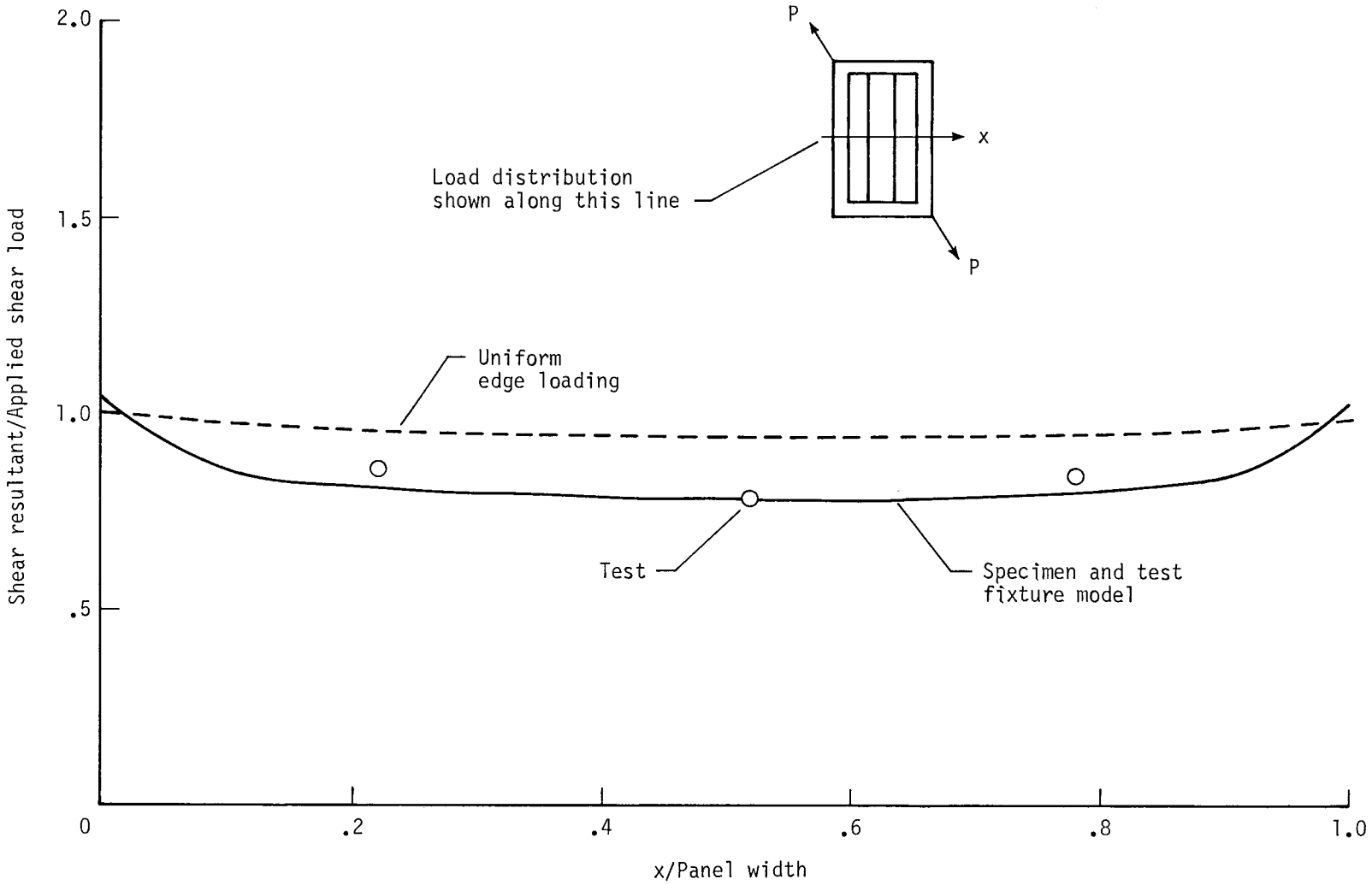

Figure 10.- Shear load distribution across middle of panel.

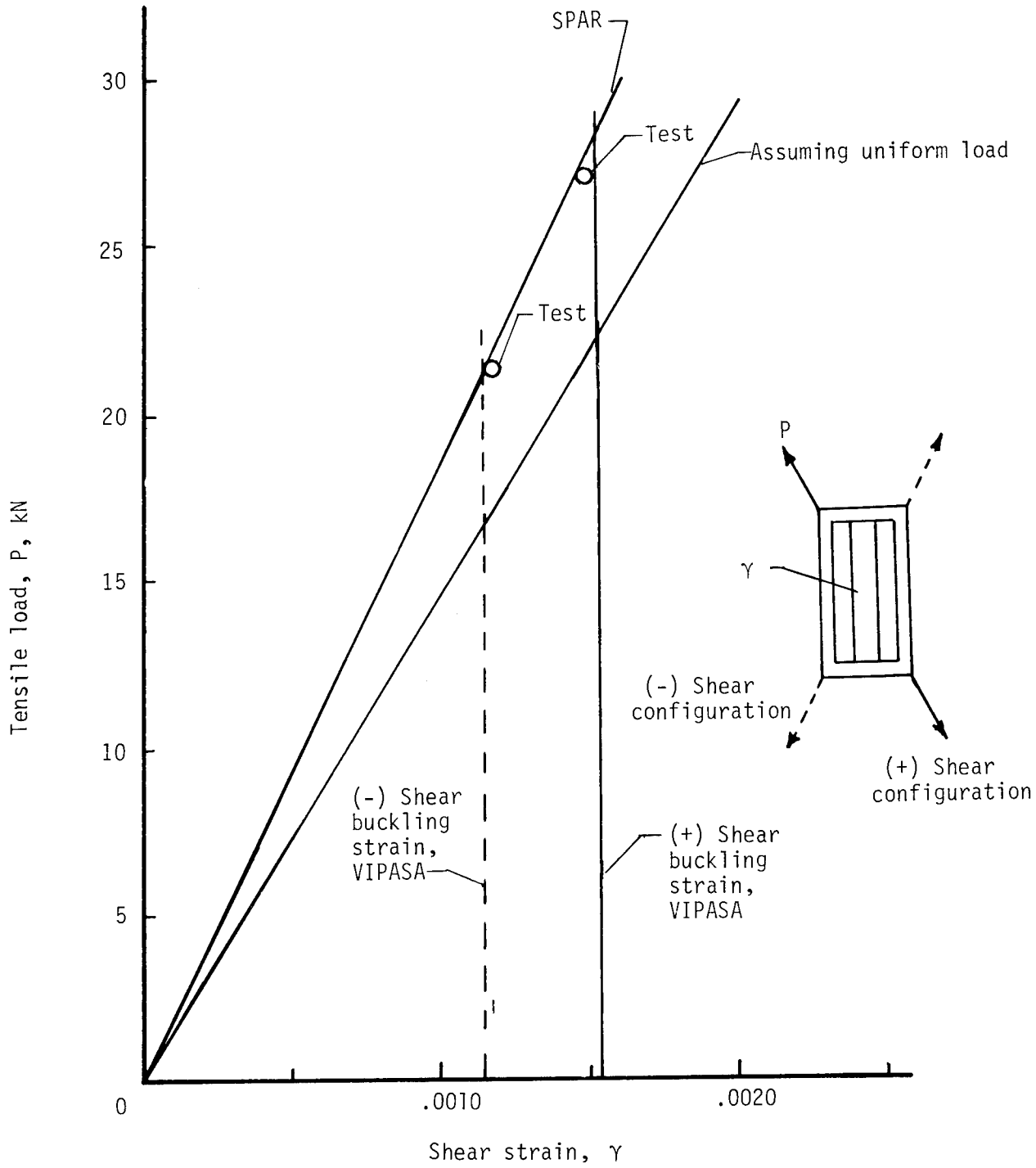

Figure 11.- Graph of tensile load applied to picture frame apparatus and amount of shear strain generated in center of panel.

1. Report No.	2. Government Accession No.	3. Recipient's Catalog No.
NASA TP-1607		

4. Title and Subtitle	5. Report Date
STRESS ANALYSIS AND BUCKLING OF J-STIFFENED GRAPHITE-EPOXY PANEL	February 1980
	6. Performing Organization Code
7. Author(s)	8. Performing Organization Report No.
Randall C. Davis	L-13256
	10. Work Unit No.
9. Performing Organization Name and Address	506-17-23-01
NASA Langley Research Center Hampton, VA 23665	11. Contract or Grant No.
	13. Type of Report and Period Covered
12. Sponsoring Agency Name and Address	Technical Paper
National Aeronautics and Space Administration Washington, DC 20546	14. Sponsoring Agency Code

15. Supplementary Notes

16. Abstract

A graphite-epoxy shear panel with bonded-on J-stiffeners has been investigated. The panel was loaded to buckling in a picture frame shear test. Two finite element models, each of which included the doubler material bonded to the panel skin under the stiffeners and at the panel edges, were used to make a stress analysis of the panel. The shear load distributions in the panel from two commonly used boundary conditions, applied shear load and applied displacement, were compared with the results from one of the finite element models that included the picture frame test fixture. Analysis results show that the use of bonded doubler material under the stiffeners and at the panel edges in conjunction with the test fixture loading produces a highly nonuniform shear load distribution in the panel. The analytical results were verified by comparison with strain and buckling results from the well-controlled laboratory test of the panel.

17. Key Words (Suggested by Author(s))		18. Distribution Statement
Composites	Picture frame	Unclassified - Unlimited
Shear panel	Shear tests	
Buckling	Bonded stiffeners	
Graphite-epoxy		Subject Category 39

19. Security Classif. (of this report)	20. Security Classif. (of this page)	21. No. of Pages	22. Price*
Unclassified	Unclassified	20	$4.00

* For sale by the National Technical Information Service, Springfield, Virginia 22161

NASA-Langley, 1980